Wills Eye Hospital Papers

Wills Eye Hospital

9-1-2021

Cross-Sectional Analysis of Baseline Visual Parameters in Subjects Recruited Into the RESCUE and REVERSE ND4-LHON Gene Therapy Studies

Mark Moster

Robert C Sergott

Nancy J Newman

Patrick Yu-Wai-Man

Valerio Carelli

See next page for additional authors

Authors

Mark Moster, Robert C Sergott, Nancy J Newman, Patrick Yu-Wai-Man, Valerio Carelli, Molly Scannell Bryan, Gerard Smits, Valérie Biousse, Catherine Vignal-Clermont, Thomas Klopstock, Alfredo A Sadun, Adam A. DeBusk, Michele Carbonelli, Rabih Hage, Siegfried Priglinger, Rustum Karanjia, Laure Blouin, Magali Taiel, Barrett Katz, and José Alain Sahel

OPEN

Cross-Sectional Analysis of Baseline Visual Parameters in Subjects Recruited Into the RESCUE and REVERSE *ND4*-LHON Gene Therapy Studies

Mark L. Moster, MD, Robert C. Sergott, MD, Nancy J. Newman, MD,
Patrick Yu-Wai-Man, MD, PhD, Valerio Carelli, MD, PhD, Molly Scannell Bryan, PhD,
Gerard Smits, PhD, Valérie Biousse, MD, Catherine Vignal-Clermont, MD,
Thomas Klopstock, MD, Alfredo A. Sadun, MD, PhD, Adam A. DeBusk, MD,
Michele Carbonelli, MD, Rabih Hage, MD, Siegfried Priglinger, MD, PhD,
Rustum Karanjia, MD, PhD, Laure Blouin, Magali Taiel, MD, Barrett Katz, MD,
José Alain Sahel, MD, PhD, for the LHON study group

Objective: This report presents a cross-sectional analysis of the baseline characteristics of subjects with Leber hereditary optic neuropathy enrolled in the gene therapy trials RESCUE and REVERSE, to illustrate the evolution of visual parameters over the first year after vision loss.
Methods: RESCUE and REVERSE were 2 phase III clinical trials designed to assess the efficacy of rAAV2/2-*ND4* gene therapy in *ND4*-LHON subjects. At enrollment, subjects had vision loss for ≤6 months in RESCUE, and between 6 and 12 months in REVERSE. Functional visual parameters (best-corrected visual acuity [BCVA], contrast sensitivity [CS], and Humphrey Visual Field [HVF]) and structural parameters assessed by spectral-domain optical coherence tomography were analyzed in both cohorts before treatment. The cross-sectional analysis of functional and anatomic parameters included the baseline values collected in all eyes at 2 different visits (Screening and Inclusion).
Results: Seventy-six subjects were included in total, 39 in RESCUE and 37 in REVERSE. Mean BCVA was significantly worse in RESCUE subjects compared with REVERSE subjects (1.29 and 1.61 LogMAR respectively, $P = 0.0029$). Similarly, mean CS and HVF were significantly more impaired in REVERSE vs RESCUE subjects ($P < 0.005$). The cross-sectional analysis showed that the monthly decrease in BCVA, ganglion cell layer macular volume, and retinal nerve fiber layer thickness was much more pronounced in the first 6 months after onset (+0.24 LogMAR, -0.06 mm³, and -6.00 μm respectively) than between 6 and 12 months after onset (+0.02 LogMAR, -0.01 mm³, and -0.43 μm respectively).
Conclusion: LHON progresses rapidly in the first months following onset during the subacute phase, followed by relative stabilization during the dynamic phase.

Leber hereditary optic neuropathy (LHON) is a maternally inherited blinding bilateral optic neuropathy caused by mitochondrial DNA (mtDNA) missense point mutations affecting complex I in the mitochondrial respiratory chain (1,2), resulting in selective dysfunction and subsequent apoptotic loss of retinal ganglion cells (RGCs) (3,4). LHON is considered the most common disorder caused by a mutation of the mitochondrial DNA (5). It typically affects mostly young men causing painless, loss of central vision that ultimately evolves into profound visual impairment (2–8). Eyes are affected sequentially in 50%–75% of cases, with the second eye involved within weeks or months after the first. An initial *subacute phase*, lasting approximately the first 6 months after onset, is characterized by a fairly rapid deterioration of visual function (2). Once a nadir is reached, visual acuity stabilizes, but other parameters, in particular optical coherence tomography (OCT) measurements of retinal layer thickness, will still evolve, defining a *dynamic phase* over the next 6 months. About one year after disease onset, the clinical picture enters a *chronic phase* of relative stability (2). Usually, visual prognosis is poor and most subjects reach acuities worse than 20/200 (2–4,6). The most common (75%) and most severe clinical form of LHON is caused by the m.11778G>A point mutation in the mtDNA gene encoding nicotinamide adenine dinucleotide hydride dehydrogenase protein subunit 4 (ND4) (1–4,6). A recent meta-analysis of reports on the natural history of LHON in subjects 15 years and older carrying the m.11778G>A mutation established that spontaneous recovery of meaningful visual acuity occurs in 11% of patients (9).

Recent advances in molecular biology allow for viral transduction of affected RGCs, allotopic expression of the

ND4 wild-type protein from the nucleus and its co-translocation into the mitochondrial matrix to complement the mutant protein, offering the promise of restoration of vision (10–13). rAAV2/2-*ND4* is such a gene therapy administered as an intravitreal injection (IVT) for the treatment of LHON caused by the m.11778G>A mutation. Treatment with rAAV2/2-*ND4* has been shown to be safe and well tolerated in early-phase and phase III clinical trials (14–16).

RESCUE (NCT02652767) and REVERSE (NCT02652780) were 2 Phase III clinical trials that investigated the efficacy of rAAV2/2-*ND4* in LHON subjects confirmed to carry the m.11778G>A mutation, and with time since onset of vision loss ≤6 months in RESCUE, and between 6 months and 1 year in REVERSE. In this report, we present the baseline characteristics of LHON subjects enrolled in RESCUE and REVERSE, including best-corrected visual acuity (BCVA), contrast sensitivity (CS), Humphrey Visual Field (HVF), and structural parameters assessed by spectral-domain optical coherence tomography (SD-OCT). Using cross-sectional analysis of functional and anatomic parameters ascertained at the baseline of different timepoints, we explore the correlations between duration of vision loss and these parameters before any treatment administration.

METHODS

Study Design

RESCUE and REVERSE (ClinicalTrial.gov NCT02652767 and NCT026527080) (15,16) were 2 randomized, double-masked, sham-controlled, multicenter, international, pivotal

Departments of Neurology and Ophthalmology (MLM, RCS, AAD), Wills Eye Hospital and Thomas Jefferson University, Philadelphia, Pennsylvania; Departments of Ophthalmology (NJN, VB), Neurology and Neurological Surgery, Emory University School of Medicine, Atlanta, Georgia; Cambridge Centre for Brain Repair and MRC Mitochondrial Biology Unit (PY-W-M), Department of Clinical Neurosciences, University of Cambridge, Cambridge, United Kingdom; Cambridge Eye Unit (PY-W-M), Addenbrooke's Hospital, Cambridge University Hospitals, Cambridge, United Kingdom; Moorfields Eye Hospital (PY-W-M), London, United Kingdom; UCL Institute of Ophthalmology (PY-W-M), University College London, London, United Kingdom; IRCCS Istituto Delle Scienze Neurologiche di Bologna (VC, MC), UOC Clinica Neurologica, Bologna, Italy; Unit of Neurology (VC), Department of Biomedical and Neuromotor Sciences (DIBINEM), University of Bologna, Bologna, Italy; Institute of Health Research and Policy (MSB), University of Illinois, Chicago, Chicago, Illinois; Statistics Consultant (GS), GenSight Biologics, CaliforniaDepartment of Neuro Ophthalmology and Emergencies (CV-C, RH), Rothschild Foundation Hospital, Paris, France; Centre Hospitalier National D'Ophtalmologie des Quinze Vingts (CV-C, RH), Paris, France; Department of Neurology (TK), Friedrich-Baur-Institute, University Hospital, LMU Munich, Munich, Germany; German Center for Neurodegenerative Diseases (DZNE) (TK), Munich, Germany; Munich Cluster for Systems Neurology (SyNergy) (TK), Munich, Germany; Doheny Eye Center UCLA (AAS, RK), Department of Ophthalmology David Geffen School of Medicine at UCLA, Doheny Eye Institute, Los Angeles, CaliforniaDepartment of Ophthalmology (SP), University Hospital, LMU Munich, Munich, Germany; Department of Ophthalmology (RK), University of Ottawa Eye Institute, Ottawa Canada; GenSight Biologics (LB, MT), Paris, France; Medical Consultant (BK), GenSight Biologics; Sorbonne Université (JAS), INSERM, CNRS, Institut de La Vision, 75012 Paris, France; Fondation Ophtalmologique A. de Rothschild (JAS), 25-29 Rue Manin, Paris; Department of Ophthalmology (JAS), the University of Pittsburgh School of Medicine, PittsburghCHNO des Quinze-Vingts (JAS), Institut Hospitalo-Universitaire FOReSIGHT, INSERM-DGOS CIC 1423, Paris, France.

clinical trials to evaluate the efficacy of a single IVT of rAAV2/2-*ND4* in subjects with LHON secondary to the m.11778G>A mutation. Both protocols were prospectively reviewed and approved by independent ethics committees (the London—West London & Gene Therapy Advisory Committee Research Ethics Committee in the United Kingdom; the *Comité de Protection des Personnes* in France; the *Ethikkommission der Medizinischen Fakultät der Ludwig-Maximilians Universität München* in Germany; the *Comitato Etico Interaziendale Bologna-Imola* in Italy; the Wills Eye Hospital Institutional Review Board, the Emory University Institutional Review Board, and the University of California Los Angeles General Campus Institutional Review Board in the United States), were conducted in accordance with the principles and requirements of the International Conference on Harmonization Good Clinical Practice and adhered to the Declaration of Helsinki. Informed consent was obtained from patients before inclusion in trials.

Study Population

The recruitment period for REVERSE and RESCUE was from February 2016 to March and August 2017, respectively.

Inclusion Criteria

To be included in either study, LHON subjects had to harbor the m.11778G>A mutation, be at least 15 years old at enrollment, and have vision of count fingers or better in both eyes. In RESCUE, one or both eyes could be affected by vision loss provided the duration of vision loss was ≤180 days in the affected eye(s) at screening. In REVERSE, both eyes had to be affected by vision loss for 181–365 days at time of screening. The screening visit occurred 28 to 1 day(s) before the inclusion visit, which was performed the day before IVT administration. Documented genotyping was required to confirm the presence of the m.11778G>A mutation in the MT-*ND4* gene and the absence of other primary LHON-associated mutations (*MT-ND1* or *MT-ND6*). Whole mitochondrial genome sequencing was not performed. The subjects recruited into RESCUE and REVERSE had classical LHON phenotypes and nuclear genome sequencing was not specifically requested to exclude other optic atrophy genes.

Exclusion Criteria

The exclusion criteria included any previously known inherited retinal or optic nerve conditions. Additional exclusion criteria were previous treatment with an ocular gene therapy product, glaucoma, optic neuropathy other than LHON, history of amblyopia, previous vitrectomy in either eye, or ocular surgery within 90 days. Prior use of idebenone was required to have ceased at least 7 days before inclusion. This was believed to be a sufficient

length of time because idebenone is rapidly absorbed, with an average plasma half-life of about 15 hours (17).

Assessments at Baseline

Demographic characteristics were collected before treatment, along with visual function and anatomic parameters. Ophthalmic evaluations included BCVA using the Early-Treatment Diabetic Retinopathy Study (ETDRS) charts at 1 or 4 m, assessment of CS using the Pelli–Robson chart, HVF 30-2 testing, Farnsworth-Munsell 100-Hue Color Vision testing, slit-lamp microscopy, Goldmann applanation tonometry, funduscopy, SD-OCT, and color fundus photography. The predefined baseline for functional visual parameters (BCVA, CS, HVF, color vision) was the last available assessment before treatment; for anatomic metrics (OCT), the baseline was defined as the average of values measured at screening and inclusion visits. In this manuscript, to better characterize the evolution of these previous parameters before treatment, we have included the values both at screening (within one month before inclusion) and at inclusion (one day before treatment).

When subjects could not read any letters on the ETDRS chart, they were asked to count the assessor's fingers or to detect hand motion. An off-chart Snellen equivalent was derived using both the distance at which the assessment was made and the size of the assessor's fingers, as described by Karanjia et al (18) (this method was also adapted to hand motion visual acuity), then was converted into a LogMAR value. Light perception and no light perception visual acuities were assigned a value of 4.0 and 4.5 LogMAR, respectively.

CS—the reciprocal of contrast threshold—was measured using the Pelli–Robson chart at 1 m, performed according to test instructions and expressed as a logarithm (LogCS) (19). Subjects who could not read more than one letter of the first triplet on the Pelli–Robson chart were considered off-chart, and the value assigned according to the statistical analysis plan was the worst possible score (0 LogCS).

For visual field assessment, the standardized automated procedure HVF 30-2, Central Threshold, SITA-FAST was performed using the HVF Analyzer II. A reading center masked to treatment allocation (Optic Nerve Research Center, William H Annesley Jr. EyeBrain Center, Thomas Jefferson University) performed quality control, analysis, and interpretation of all OCT and HVF data. The HVF test was repeated if considered unreliable by the reading center (i.e., fixation losses ≥15%, false positive errors ≥20%, or false negative errors ≥33%).

SD-OCT was performed with the Spectralis OCT (Heidelberg Engineering). Among other parameters, retinal nerve fiber layer (RNFL) and ganglion cell layer (GCL) were measured for the optic nerve and posterior pole per standard protocols included in the Spectralis software. At prespecified visits, certified technicians performed one "Optic Nerve Head—Radial Scan and Concentric Circle

Scan" (ONH-RC) and one "Posterior Pole N Scan" (PPo-leN) for each eye, after maximal dilation. The OCT assessments were performed using triplicate scans of high quality (Q values >20). Borders of the retinal layers were manually adjusted when algorithm errors were detected.

HVF and OCT analyses were also masked to BCVA, CS, ophthalmic examinations, and duration of visual loss.

Statistical Approach

Statistical analyses were performed using SAS.

Software version 9.4 (SAS Institute, Cary, NC).

Summary statistics for continuous variables were described using N, mean standardization, and range. This approach was applied both to independent data (e.g., age) and to dependent data representing both eyes from the same subject. Numbers and percentages were described in the same manner, representing both independent and dependent summaries. Analyses of dependent data were performed using a mixed-effects analysis of variance and the covariance between paired eyes was determined by the model.

The monthly rates of loss of visual function and retinal anatomy were estimated based on a linear fit from mixed-effect models of individual data points collected at baseline and plotted relative to onset of vision loss. They represent the slope of the linear fit derived from the scatterplot of individual data for a given visual parameter over time since onset. The eyes with no vision loss were included in the regression model, with a duration of vision loss set to zero.

A locally estimated scatterplot smoothing (LOESS) nonparametric, local regression model was used on the individual data points. The resulting curve depicting the evolution of visual and anatomical parameters over time was based on a series of polynomial regressions around each data point. The regressions used a limited look back and look forward, giving distant points less weight.

RESULTS

Demographic Characteristics

Seventy-six subjects with LHON confirmed to carry the m.11778G>A mutation were included from both studies, 39 from RESCUE and 37 from REVERSE. Participants were on average 35 years of age and mostly men (61 (80.2%) of 76 patients) (Table 1). Mean age and gender distribution were similar in both trials. Overall, 26 (34.2%) of 76 subjects reported simultaneous bilateral onset of vision loss.

Duration of Vision Loss

As expected from the study design, the mean duration of vision loss was shorter in RESCUE (3.7 months/112.1 days) than in REVERSE (8.9 months/271.0 days) (Table 1). This difference was statistically significant ($P < 0.0001$).

Visual Function: BCVA, CS, and HVF

Best-Corrected Visual Acuity

At baseline, BCVA was on average more preserved in RESCUE subjects compared with REVERSE subjects, a difference that was statistically significant (1.29 LogMAR [20/400 Snellen] and 1.61 LogMAR [20/800 Snellen] respectively, $P = 0.0029$) (Table 1). In RESCUE, 4 eyes had normal visual acuity ($\geq$20/20) at baseline, as monocular vision loss was allowed for inclusion in this study (see **Supplemental Digital Content 1**, **Supplementary Table 1**, http://links.lww.com/WNO/A484).

BCVA values, collected and analyzed per eye in both studies at screening and inclusion (for a total of 304 observations in 152 eyes), were grouped, averaged and plotted as a function of duration of vision loss (Fig. 1A). Cross-sectional BCVA values substantially worsened in the first 8 months ($\sim$250 days) after onset of vision loss, and were globally off-chart after 8 months of vision loss. These results were validated by a nonparametric LOESS regression model (see **Supplemental Digital Content 2**, **Supplementary Figure 3**, http://links.lww.com/WNO/A475).

Linear regression on individual data points showed that each additional month after symptom onset was associated with a +0.24 logMAR difference in BCVA during the 0–6-month period, compared with a +0.02 logMAR difference during the 6–12 month period (Table 2).

Contrast Sensitivity

At baseline, CS was on average more preserved in RESCUE subjects compared with REVERSE subjects, a difference that was statistically significant (0.62 LogCS and 0.30 LogCS respectively, $P = 0.0031$) (Table 1). In REVERSE, 27/74 (36.5%) eyes were off-chart for CS at inclusion (i.e., these eyes could not correctly read 2 letters at the maximum contrast possible on the Pelli–Robson chart). In RESCUE, all eyes were on-chart for CS at inclusion. As per protocol, the value assigned to off-chart eyes was the worst possible score (0 LogCS), enabling the inclusion of all eyes in CS analyses.

Baseline CS values collected in both studies were averaged and plotted as a function of duration of vision loss (Fig. 1B). Cross-sectional CS values declined similarly as BCVA measures in the first 8 months ($\sim$250 days) of vision loss, then were globally around 0.3 LogCS (equivalent to a detection threshold of 50% contrast when normal control subjects can detect on average a 1.6% contrast [1.8 LogCS]) (20). These results were validated by a nonparametric LOESS regression model (see **Supplemental Digital Content 3**, **Supplementary Figure 4**, http://links.lww.com/WNO/A476).

Linear regression on individual data points showed that each additional month after symptom onset was associated with a −0.15 LogCS difference in CS during the 0–6 month period, compared to a +0.01 LogCS difference during the 6–12 month period (Table 2).

TABLE 1. Demographic characteristics—Visual function and retinal anatomy before treatment

	All	RESCUE	REVERSE	P*
N subjects	76	39	37	
N males (%)	61 (80.2%)	32 (82.0%)	29 (78.4%)	0.7770
Age (years)				
Mean (SD)	35.3 (15.3)	36.3 (15.5)	34.2 (15.2)	0.5451
Min; max	15; 69	15; 69	15; 67	
Simultaneous bilateral onset				
N subjects (%)	26 (34.2%)	19 (48.7%)	7 (18.9%)	0.0062
Duration of vision loss (days)†				
N eyes	147	73	74	
Mean (SD)	192.1 (95.0)	112.1 (42.8)	271.0 (59.5)	<0.0001
Min; max	24; 364	24; 179	181; 364	
N eyes	152	78	74	
BCVA (LogMAR)				
Mean (SD)	1.45 (0.54)	1.29 (0.56)	1.61 (0.46)	0.0029
Min; max	−0.20; 3.17	−0.20; 2.51	0.70; 3.17	
Contrast sensitivity (LogCS)				
Mean (SD)	0.46 (0.51)	0.62 (0.54)	0.30 (0.43)	0.0031
Min; max	0; 1.65	0; 1.65	0; 1.50	
HVF mean deviation (dB)‡				
Mean (SD)	−24.4 (10.9)	−19.9 (12.1)	−29.0 (7.2)	0.0039
Min; max	−34.7; −1.9	−34.7; −1.9	−34.6; −5.1	
HVF pattern SD (dB)‡				
Mean (SD)	5.9 (3.4)	6.5 (3.6)	5.3 (3.1)	0.1865
Min; max	1.3; 13.0	1.3; 13.0	1.7; 12.6	
GCL macular volume (mm^3)				
Mean (SD)	0.63 (0.16)	0.73 (0.17)	0.53 (0.066)	<0.0001
Min; max	0.42; 1.28	0.50; 1.28	0.42; 0.72	
ETDRS total macular volume (mm^3)				
Mean (SD)	8.12 (0.51)	8.40 (0.47)	7.83 (0.36)	<0.0001
Min; max	6.54; 9.58	7.54; 9.58	6.54; 8.75	
RNFL temporal quadrant (μm)				
Mean (SD)	39.2 (19.2)	49.6 (20.9)	28.2 (8.0)	<0.0001
Min; max	13.5; 147.5	24.5; 147.5	13.5; 62.5	
PMB RNFL thickness (μm)				
Mean (SD)	29.2 (12.7)	34.8 (14.4)	23.4 (6.7)	<0.0001
Min; max	1.5; 123.0	21.0; 123.0	1.5; 39.5	
Average RNFL thickness (μm)				
Mean (SD)	84.8 (23.3)	99.1 (18.2)	69.7 (18.1)	<0.0001
Min; max	39.5; 162.0	47.0; 162.0	39.5; 116.5	

Means were calculated based on data collected at inclusion for BCVA, CS, and HVF. For OCT parameters, the means were calculated based on the average values of data collected at screening and inclusion.

*P-values compare results from RESCUE and REVERSE.

†The onset of vision loss was based on patient testimony; the duration of vision loss was assessed at screening in eyes with vision loss perceived by the patient. In RESCUE, 4 eyes had no vision loss and one eye had vision loss not perceived by the patient (LogMAR +0.1 [20/25]); these 5 eyes were not included in the calculation of mean duration of vision loss.

‡Means were calculated in 65 eyes with reliable HVF test results at study inclusion (33 in RESCUE and 32 in REVERSE).

Mean Deviation of HVF

At baseline, 65 (42.8%) of 152 eyes had reliable HVF 30-2 test results: 33 (42.3%) of 78 eyes in RESCUE and 32 (43.2%) of 74 eyes in REVERSE. The average mean deviation of HVF 30-2 was significantly worse in REVERSE subjects compared with RESCUE subjects, with −29.0 dB and −19.9 dB, respectively (P = 0.0039) (Table 1).

Mean deviation (MD) values from reliable HVF tests, collected in both studies at screening and inclusion (for a total of 128 reliable observations in 110 eyes), were grouped, averaged, and plotted as a function of duration of vision loss (Fig. 1C). Similar to BCVA and CS, cross-sectional HVF MD values substantially worsened in the first 8 months (∼250 days) after onset of vision loss. These results were validated by a nonparametric LOESS regression model (see **Supplemental Digital Content 4**, **Supplementary Figure 5**, http://links.lww.com/WNO/A477).

Linear regression on individual data points showed that each additional month after symptom onset was associated with a −2.55 dB difference in HVF MD during the 0–6 month period, compared to a +0.40 dB difference during the 6–12 month period (Table 2).
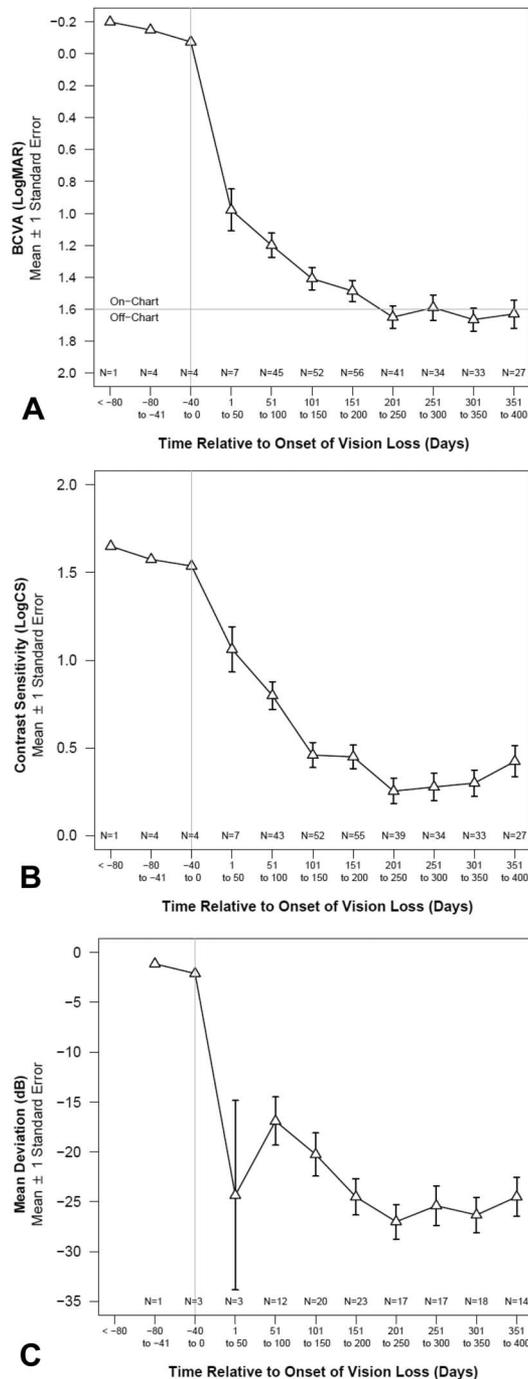
FIG. 1. Visual function parameters up to one year after onset of vision loss in subjects with LHON harboring the m.11778G>A mutation. N: number of observations pooled together to calculate the means. Individual values were collected at screening and inclusion, then grouped and averaged by time since onset of vision loss. Because of a very low number of observations available before onset of vision loss, no standard error was calculated. **A**. Best-corrected visual acuity, **B**. contrast sensitivity, **C**. HVF mean deviation. HVF, Humphrey Visual Field; LHON, Leber hereditary optic neuropathy.

Pattern Standard Deviation of HVF

At baseline, the average pattern standard deviation (PSD) of HVF 30-2 was similar in RESCUE and REVERSE eyes, with 6.5 and 5.3 dB, respectively (P = 0.1865) (Table 1).

PSD values from reliable HVF tests, collected in both studies at screening and inclusion (for a total of 128 reliable observations in 110 eyes), were grouped, averaged, and plotted as a function of duration of vision loss (see **Supplemental Digital Content 5**, **Supplementary Figure 1B**, http://links.lww.com/WNO/A473). Cross-sectional PSD values increased during the first 100 days after onset of vision loss, and then decreased. These results were validated by a nonparametric LOESS regression model (see **Supplemental Digital Content 6**, Supplementary Figure 6, http://links.lww.com/WNO/A478).

Linear regression on individual data points showed that each additional month after symptom onset was associated with a +0.44 dB difference in HVF PSD during the 0–6-month period, compared with a −0.30 dB difference during the 6–12 month period (Table 2).

Retinal Anatomy: SD-OCT Assessment

The analyses of retinal anatomy focused on the thickness and volume of the retinal layers most affected in LHON subjects, the GCL and RNFL. Both these retinal parameters showed more advanced loss in REVERSE subjects compared with RESCUE subjects ($P < 0.0001$) (Table 1). The average GCL macular volume was 0.530 mm^3 vs 0.734 mm^3 in RESCUE and REVERSE, respectively, and the average RNFL thickness in the temporal quadrant was 28.2 μm vs 49.6 μm, respectively.

Baseline OCT parameters collected in both studies were averaged and plotted as a function of duration of vision loss (Fig. 2 and see **Supplemental Digital Content 5**, **Supplementary Figure 1A, 1C**, http://links.lww.com/WNO/A473). All cross-sectional OCT parameters dramatically deteriorated in the first 8 months (~250 days) after onset of vision loss and were then globally stable. These results were validated by a nonparametric LOESS regression models (see **Supplemental Digital Contents 7–11**, **Supplementary Figures 7–11**, http://links.lww.com/WNO/A479, http://links.lww.com/WNO/A480, http://links.lww.com/WNO/A481, http://links.lww.com/WNO/A482, http://links.lww.com/WNO/A483).

Based on cross-sectional data, linear regression on individual data points showed that, in the first 6 months after onset of vision loss, the monthly structural loss was on average: −0.06 mm^3 of GCL macular volume, −0.07 mm^3 of ETDRS total macular volume, −6.00 μm of RNFL thickness in the temporal quadrant, −5.76 μm of RNFL thickness in the papillomacular bundle, and −3.06 μm of average RNFL thickness (Table 2).

TABLE 2. Monthly rates of change in visual parameters

	Monthly Rate Estimate		
	All	RESCUE	REVERSE
BCVA (LogMAR)			
Estimate	+0.08	+0.24	+0.02
95% CI	0.061 to 0.104	0.201 to 0.278	−0.013 to 0.052
P-value	<0.0001	<0.0001	0.2503
CS (LogCS)			
Estimate	−0.05	−0.15	+0.01
95% CI	−0.073 to −0.032	−0.197 to 0.111	−0.014 to 0.034
P-value	<0.0001	<0.0001	0.4235
HVF MD (dB)			
Estimate	−0.62	−2.55	+0.40
95% CI	−1.095 to −0.136	−3.863 to −1.230	−0.066 to 0.871
P-value	0.0141	0.0007	0.1000
HVF PSD (dB)			
Estimate	−0.08	+0.44	−0.30
95% CI	−0.283 to 0.116	−0.170 to 1.059	−0.502 to −0.098
P-value	0.4159	0.1669	0.0059
GCL macular volume (mm^3)			
Estimate	−0.03	−0.06	−0.01
95% CI	−0.033 to −0.024	−0.068 to −0.053	−0.013 to −0.003
P-value	<0.0001	<0.0001	0.0023
ETDRS total macular volume (mm^3)			
Estimate	−0.04	−0.07	−0.01
95% CI	−0.052 to −0.026	−0.087 to −0.049	−0.028 to 0.011
P-value	<0.0001	<0.0001	0.3869
RNFL temporal quadrant (μm)			
Estimate	−2.71	−6.00	−0.43
95% CI	−3.269 to −2.160	−7.174 to −4.830	−0.848 to −0.005
P-value	<0.0001	<0.0001	0.0502
PMB RNFL (μm)			
Estimate	−2.06	−5.76	−0.02
95% CI	−2.552 to −1.561	−6.846 to −4.673	−0.616 to 0.569
P-value	<0.0001	<0.0001	0.9392
Average RNFL (μm)			
Estimate	−3.25	−3.06	−2.49
95% CI	−3.890 to −2.611	−4.493 to −1.635	−3.135 to −1.844
P-value	<0.0001	<0.0001	<0.0001

BCVA, best-corrected visual acuity; CS, contrast sensitivity; CI, confidence interval; ETDRS, Early-Treatment Diabetic Retinopathy Study; GCL, ganglion cell layer; HVF, Humphrey visual field; MD, mean deviation; PMB, papillomacular bundle; PSD, pattern SD; RNFL, retinal nerve fiber layer.

Eyes Unaffected by BCVA Loss

Four eyes were not affected by BCVA loss at the time of study enrollment in RESCUE (see **Supplemental Digital Content 1**, **Supplementary Table 1**, http://links.lww.com/WNO/A484). Although they all had normal BCVA (≤0.0 LogMAR), they were already showing signs of loss of CS, with values below 1.8 LogCS. When HVF tests were reliable, MD values ranged from −2.4 to −1.14 dB and PSD values ranged from 1.29 to 1.87 dB. In the 4 eyes assessed before onset of vision loss, an increase of thickness/volume was observed in all retinal layers of interest: GCL, RNFL in the temporal quadrant and papillomacular bundle, RNFL average thickness, and ETDRS total macular volume. A detailed description of these 4 eyes, including fundus photographs, HVFs, peripapillary RNFL thickness per quadrant, and GCL macular thickness and volume, is provided in **Supplemental Digital Content 12**, (see **Supplementary Figure 2**, http://links.lww.com/WNO/A474).

CONCLUSION

We present a large data set of retinal anatomic measurements and visual function ascertained during the first year following visual loss in LHON subjects carrying the m.11778G>A mutation. Our cross-sectional data collection was performed at screening (≤1 month pretreatment) and inclusion (1 day pretreatment), shortly before patients received gene therapy in one eye. As such, this report does not constitute a longitudinal study of the
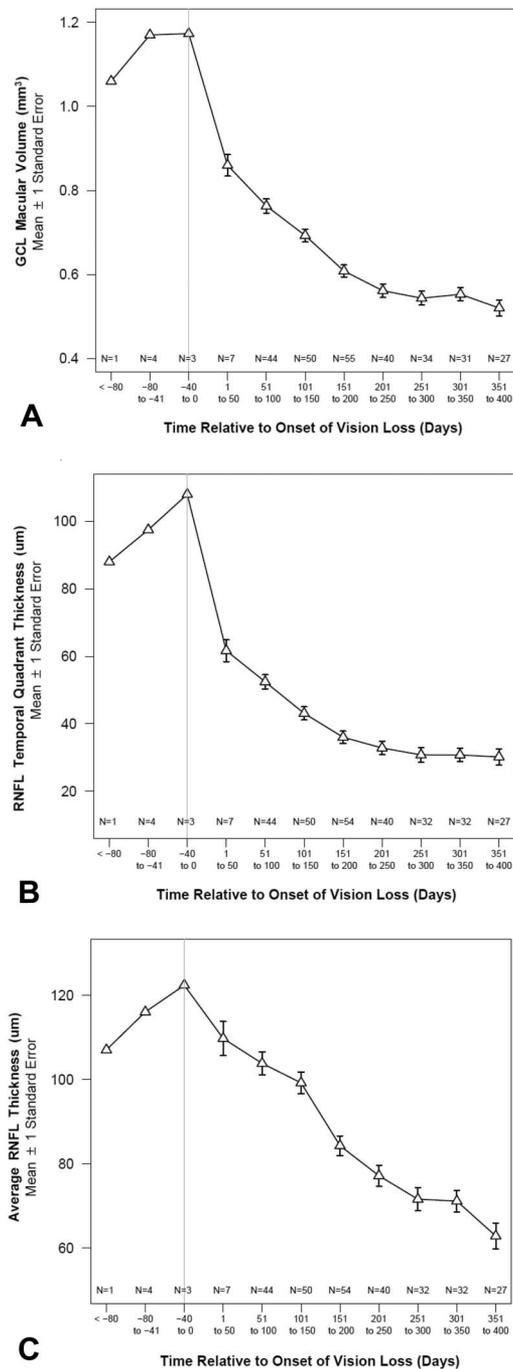
FIG. 2. Retinal parameters up to one year after onset of vision loss in subjects with LHON harboring the m.11778G>A mutation. N: number of observations pooled together to calculate the means. Individual values were collected at screening and inclusion, then grouped and averaged by time since onset of vision loss. Because of a very low number of observations available before onset of vision loss, no standard error was calculated. **A**. Ganglion cell layer macular volume, **B**. Retinal nerve fiber layer (RNFL) temporal quadrant thickness, **C**. Average RNFL thickness.

natural history of untreated individuals with LHON. Nonetheless, since enrollment in the RESCUE and REVERSE clinical trials spanned the course of one year from onset of vision loss, the collected data allowed for cross-sectional analysis of the natural history of LHON over the first year after onset.

Our findings are in keeping with the evolution of the disease process in LHON. Unsurprisingly, longer durations of vision loss were associated with worse retinal anatomy parameters and visual function. All cross-sectional functional (BCVA, CS, and HVF) and retinal anatomic measurements (GCL macular volume, RNFL thickness, and total macular volume) drastically worsened in approximately the first 8 months after onset, and were then globally stable. The deterioration of OCT anatomic parameters lagged slightly behind the visual functions. However, pathological thickening of these retinal structures before visual loss and in the early stages of visual decline, as particularly demonstrated in those patients with presymptomatic second eyes at baseline, may have contributed partly to this delay in measurable deterioration.

The loss of function and retinal structure was more pronounced at later cross-sectional data points and ultimately correlated with the degree of visual acuity deficit. In 2017, a consortium of LHON experts established 3 stages in the disease progression: the "subacute" phase, the "dynamic" phase, and the "chronic" phase (2). The international consensus statement on the clinical and therapeutic management of LHON defined the first 6 months after onset as the subacute or acute phase, depending on how rapidly the loss of central vision evolves. Visual acuity usually stabilizes between 4 and 6 months after onset, but other clinical metrics such as visual fields and OCT measurements may still evolve in the dynamic phase, up to 12 months after onset. One year after onset, visual function and retinal anatomy should have plateaued and the patient typically transitions into the chronic stage of the disease (2). Our results align with the description of the subacute and dynamic phases observed over the first year of the disease. In this cross-sectional analysis, BCVA stabilized a bit later at approximately 8 months after onset.

The demographic characteristics of LHON subjects were similar between the RESCUE and REVERSE trials. The cohorts recruited for both studies were aligned with a typical LHON population as regards gender and age distributions (80% men, mean age at onset 35 years old) (2–4,6,9). Based on protocol inclusion criteria, only the average duration of vision loss at enrollment was significantly different between studies. As expected, this difference in duration of vision loss was associated with worse visual functions and anatomic structural parameters in the REVERSE population, compared to RESCUE.

One year after onset of vision loss, the final average BCVA was off chart. CS followed a similar pattern of acute decline. Our cross-sectional data showed that the visual field deteriorated as well, first with the appearance of focal defects, mainly a central scotoma, which is the hallmark of LHON, resulting in an increase in PSD. Then, the overall diffuse deterioration of the visual field caused a slow decrease in PSD, as observed in eyes with more than 6 months of vision loss. Of note, only reliable HVF tests were included in this analysis, resulting in more than half of the data being excluded.

Overall, the dramatic BCVA drop reported in this cross-sectional analysis is consistent with the poor visual prognosis associated with the m.11778G>A mtDNA mutation reported in a recent natural history meta-analysis (9). Among 204 LHON subjects carrying the primary *MT-ND4* mutation and aged 15 or older at onset, spontaneous recovery was detected in only 11% of cases (9).

Based on cross-sectional data, our results support previous work reporting relatively rapid loss of retinal tissues in the first few months following onset of vision loss in LHON patients (21–25). The dramatic loss of tissue occurs during the subacute and dynamic phases of the disease and reaches a nadir a short time after the nadir of visual acuity. During the subacute phase, there is evidence that the thinning in the GCL occurs before the thinning in the RNFL, the average RNFL thickness being relatively stable (24). Further deterioration may remain undetected by a "floor effect" because of technical limitations of currently available OCT platforms. On the other end of the spectrum, the 4 eyes with normal visual acuity at enrollment shed light on the changes in retinal anatomy that precede the onset of BCVA loss. As previously described in other studies, assessment of key anatomic parameters showed presymptomatic increase of thickness of the RNFL, macular volume, and GCL volume, suggestive of evolving swelling heralding the imminent occurrence of visual symptoms (22,24,25). Interestingly, worsening of CS may also be a harbinger of the onset of BCVA loss, because eyes with preserved BCVA were already showing CS impairment. The occurrence of BCVA loss perhaps can be viewed as the ultimate outcome of anatomic and visual function (CS) changes that began at an earlier phase of the disease expression process (22,25). However, it should be noted that many patients in the acute phase of LHON may not have visible or demonstrable RNFL thickening (6), and, conversely, the presence of transient RNFL thickening in asymptomatic carriers who never proceed to symptomatic visual loss makes it difficult to use anatomic or functional measures as predictors of visual outcome (26,27).

The limitations of our analyses are related to the cross-sectional nature of the data, as subjects naive to LHON treatment were subsequently administered gene therapy and not followed longitudinally as untreated individuals. Thus, our reconstruction of the events occurring as the natural history during the first year after onset of visual loss is not based on the preferred prospective follow-up of individual patients, but rather on the collection of independent cross-sectional data points. However, the data assembled from these 2 trials provide a valuable landscape of the clinical characteristics of LHON patients harboring the m.11778G>A mutation in *MT-ND4*, and the cross-sectional evolution of key visual functional and anatomic parameters over one year. Our study thus broadens the characterization of LHON, and affords complementary evidence supporting the use of BCVA as the key endpoint currently available to assess the efficacy of LHON therapy (15,16).

Valerio Carelli, MD, PhD (Principal Investigator REVERSE, RESCUE), Piero Barboni, MD (Surgeon, IVT injections, REVERSE, RESCUE), Michele Carbonelli, MD (Sub-Investigator REVERSE, RESCUE), Lidia Di Vito, MD (Sub-Investigator REVERSE, RESCUE), Manuela Contin, M Sc (Pharmacist REVERSE, RESCUE), Susan Mohamed, MSc (Pharmacist REVERSE, RESCUE), Chiara La Morgia, MD, PhD (Sub-Investigator REVERSE, RESCUE), Sara Silvestri (Technician REVERSE, RESCUE); *Wills Eye Hospital and Sidney Kimmel Medical College of Thomas Jefferson University, Philadelphia, PA, USA:* Mark L. Moster, MD (Principal Investigator REVERSE, RESCUE), Robert C. Sergott, MD (Head of the Central Reading Center, Annesley EyeBrain Center [AEBC], Vickie and Jack Farber Institute for Neuroscience at Jefferson Health Partnered with Wills Eye Hospital, for REVERSE, RESCUE), Melissa SantaMaria (Associate Director—Central Reading Center AEBC), Heather Tollis (Clinical Study Manager—Central Reading Center AEBC), Adam A. De-Busk, MD (Sub-Investigator REVERSE, RESCUE), Julie A. Haller, MD (Surgeon, IVT injections, REVERSE, RESCUE); Maria Massini COT (Study Coordinator REVERSE, RESCUE).

Centre Hospitalier National d'Ophtalmologie des Quinze Vingts, Paris, France and Department of Neuro Ophthalmology and Emergencies, Rothschild Foundation Hospital, Paris, France: José A. Sahel, MD, PhD, Catherine Vignal-Clermont, MD (Principal Investigator REVERSE, RESCUE), Jean François Girmens, MD (Surgeon, IVT injections, REVERSE, RESCUE), Rabih Hage, MD (Sub-Investigator REVERSE, RESCUE)

Doheny Eye Institute/UCLA School of Medicine Los Angeles, CA, USA: Alfredo A. Sadun, MD, PhD (Principal Investigator REVERSE, RESCUE), Gad Heilweil, Rustum Karanjia, MD, PhD (Sub-Investigator), Irena Tsui.

Department of Neurology Friedrich-Baur-Institute, and Department of Ophthalmology, University Hospital, Ludwig-Maximilians-University Munich, 80336 Munich, Germany: Thomas Klopstock, MD (Principal Investigator, REVERSE, RESCUE), Claudia B. Catarino, MD (Sub-Investigator, REVERSE, RESCUE), Claudia Priglinger, MD (Sub-Investigator, REVERSE, RESCUE), Siegfried Priglinger, MD (Sub-Investigator, REVERSE, RESCUE), Günther Rudolph, MD (Sub-Investigator, REVERSE, RESCUE), Stephan Thurau, MD (Sub-Investigator, REVERSE, RESCUE), Bettina von Livonius, MD (Sub-Investigator, REVERSE, RESCUE), Daniel Muth, MD (Sub-Investigator, REVERSE, RESCUE), Armin Wolf, MD (Sub-Investigator, Surgeon, IVT injections, REVERSE, RESCUE), Jasmina Al-Tamami (Study Coordinator, REVERSE, RESCUE), Angelika Pressler (Study Coordinator, REVERSE, RESCUE), Cosima Schertler (Study Nurse, REVERSE, RESCUE). *TUMCells Interdisciplinary Center for Cellular Therapies, TUM School of Medicine, Munich, Germany:* Martin Hildebrandt, MD (Sub-Investigator, REVERSE, RESCUE), Michael Neuenhahn, MD (Sub-Investigator, REVERSE, RESCUE).

REFERENCES

1. **Wallace DC**, Singh G, Lott MT, Hodge JA, Schurr TG, Lezza AM, Elsas LJ II, Nikoskelainen EK. Mitochondrial DNA mutation associated with leber's hereditary optic neuropathy. Science. 1988;242:1427–1430.
2. **Carelli V**, Carbonelli M, de Coo IF, Kawasaki A, Klopstock T, Lagrèze WA, La Morgia C, Newman NJ, Orssaud C, Pott JWR, Sadun AA, van Everdingen J, Vignal-Clermont C, Votruba M, Yu-Wai-Man P, Barboni P. International consensus statement on the clinical and therapeutic management of Leber hereditary optic neuropathy. J Neuroophthalmol. 2017;37:371–381.
3. **Yu-Wai-Man P**, Griffiths PG, Chinnery PF. Mitochondrial optic neuropathies - disease mechanisms and therapeutic strategies. Prog Retin Eye Res. 2011;30:81–114.
4. **Yu-Wai-Man P**, Votruba M, Burté F, La Morgia C, Barboni P, Carelli V. A neurodegenerative perspective on mitochondrial optic neuropathies. Acta Neuropathol. 2016;132:789–806.
5. **Yu-Wai-Man P**, Griffiths PG, Brown DT, Howell N, Turnbull DM, Chinnery PF. The epidemiology of Leber hereditary optic neuropathy in the north east of England. Am J Hum Genet. 2003;72:333–339.
6. **Newman NJ**, Lott MT, Wallace DC. The clinical characteristics of pedigrees of Leber's hereditary optic neuropathy with the 11778 mutation. Am J Ophthalmol. 1991;111:750–762.
7. **Puomila A**, Hämäläinen P, Kivioja S, Savontaus ML, Koivumäki S, Huoponen K, Nikoskelainen E. Epidemiology and penetrance of Leber hereditary optic neuropathy in Finland. Eur J Hum Genet. 2007;15:1079–1089.
8. **Mascialino B**, Leinonen M, Meier T. Meta-analysis of the prevalence of Leber hereditary optic neuropathy mtDNA mutations in Europe. Eur J Ophthalmol. 2012;22:461–465.
9. **Newman NJ**, Carelli V, Taiel M, Yu-Wai-Man P. Visual outcomes in leber hereditary optic neuropathy patients with the m.11778G>A (MTND4) mitochondrial DNA mutation. J Neuro Ophthalmol. 2020;40:547–557.
10. **Jurkute N**, Harvey J, Yu-Wai-Man P. Treatment strategies for Leber hereditary optic neuropathy. Curr Opin Neurol. 2019;32:99–104.
11. **Guy J**, Qi X, Pallotti F, Schon EA, Manfredi G, Carelli V, Martinuzzi A, Hauswirth WW, Lewin AS. Rescue of a mitochondrial deficiency causing leber hereditary optic neuropathy. Ann Neurol. 2002;52:534–542.
12. **Ellouze S**, Augustin S, Bouaita A, Bonnet C, Simonutti M, Forster V, Picaud S, Sahel JA, Corral-Debrinski M. Optimized allotopic expression of the human mitochondrial ND4 prevents blindness in a rat model of mitochondrial dysfunction. Am J Hum Genet. 2008;83:373–387.
13. **Cwerman-Thibault H**, Augustin S, Lechauve C, Ayache J, Ellouze S, Sahel JA, Corral-Debrinski M. Nuclear expression of mitochondrial ND4 leads to the protein assembling in complex I and prevents optic atrophy and visual loss. Mol Ther Methods Clin Dev. 2015;2:15003.
14. **Vignal C**, Uretsky S, Fitoussi S, Galy A, Blouin L, Girmens JF, Bidot S, Thomasson N, Bouquet C, Valero S, Meunier S, Combal JP, Gilly B, Katz B, Sahel JA. Safety of rAAV2/2-ND4 gene therapy for leber hereditary optic neuropathy. Ophthalmology. 2018;125:945–947.
15. **Newman NJ**, Yu-Wai-Man P, Carelli V, Moster ML, Biousse V, Vignal-Clermont C, Sergott RC, Klopstock T, Sadun AA, Barboni P, DeBusk AA, Girmens JF, Rudolph G, Karanjia R, Taiel M, Blouin L, Smits G, Katz B, Sahel JA; LHON Study Group. Efficacy and safety of intravitreal gene therapy for leber hereditary optic neuropathy treated within 6 Months of disease onset. Ophthalmology. 2021:S0161-6420(20)31187-8.
16. **Yu-Wai-Man P**, Newman NJ, Carelli V, Moster ML, Biousse V, Sadun AA, Klopstock T, Vignal-Clermont C, Sergott RC, Rudolph G, La Morgia C, Karanjia R, Taiel M, Blouin L, Burguière P, Smits G, Chevalier C, Masonson H, Salermo Y, Katz B, Picaud

S, Calkins DJ, Sahel JA. Bilateral visual improvement with unilateral gene therapy injection for Leber hereditary optic neuropathy. Sci Transl Med. 2020;12:eaaz7423.

17. **Damiani E**, Yuecel R, Wallace HM. Repurposing of idebenone as a potential anti-cancer agent. Biochem J. 2019;476:245–259.

18. **Karanjia R**, Hwang TJ, Chen AF, Pouw A, Tian JJ, Chu ER, Wang MY, Tran JS, Sadun AA. Correcting finger counting to snellen acuity. Neuroophthalmology. 2016;40:219–221.

19. **Pelli DG**, Robson JG, Wilkins AJ. The design of a new letter chart for measuring contrast sensitivity. Clin Vis Sci. 1988;2:187–199.

20. **Mäntyjärvi M**, Laitinen T. Normal values for the Pelli-Robson contrast sensitivity test. J Cataract Refract Surg. 2001;27:261–266.

21. **Barboni P**, Savini G, Valentino ML, Montagna P, Cortelli P, De Negri AM, Sadun F, Bianchi S, Longanesi L, Zanini M, de Vivo A, Carelli V. Retinal nerve fiber layer evaluation by optical coherence tomography in leber's hereditary optic neuropathy. Ophthalmology. 2005;112:120–126.

22. **Barboni P**, Carbonelli M, Savini G, Ramos Cdo V, Carta A, Berezovsky A, Salomao SR, Carelli V, Sadun AA. Natural history of Leber's hereditary optic neuropathy: longitudinal analysis of the retinal nerve fiber layer by optical coherence tomography. Ophthalmology. 2010;117:623–627.

23. **Balducci N**, Savini G, Cascavilla ML, La Morgia C, Triolo G, Giglio R, Carbonelli M, Parisi V, Sadun AA, Bandello F, Carelli V, Barboni P. Macular nerve fibre and ganglion cell layer changes in acute Leber's hereditary optic neuropathy. Br J Ophthalmol. 2016;100:1232–1237.

24. **Moster SJ**, Moster ML, Scannell Bryan M, Sergott RC. Retinal ganglion cell and inner plexiform layer loss correlate with visual acuity loss in LHON: a longitudinal, segmentation OCT analysis. Invest Ophthalmol Vis Sci. 2016;57:3872–3883.

25. **Hw Hwang TJ**, Karanjia R, Moraes-Filho MN, Gale J, Tran JS, Chu ER, Salomao SR, Berezovsky A, Belfort R Jr, Moraes MN, Sadun F, DeNegri AM, La Morgia C, Barboni P, Ramos CDVF, Chicani CF, Quiros PA, Carelli V, Sadun AA. Natural history of conversion of leber's hereditary optic neuropathy: a prospective case series. Ophthalmology. 2017;124:843–850.

26. **Nikoskelainen EK**, Huoponen K, Juvonen V, Lamminen T, Nummelin K, Savontaus M-L. Ophthalmologic findings in leber hereditary optic neuropathy, with special reference to mtDNA mutations. Ophthalmology. 1996;103:504–514.

27. **Sadun F**, De Negri AM, Carelli V, Salomao SR, Berezovsky A, Andrade R, Moraes M, Passos A, Belfort R, da Rosa AB, Quiros P, Sadun AA. Ophthalmologic findings in a large pedigree of 11778/Haplogroup J Leber hereditary optic neuropathy. Am J Ophthalmol. 2004;137:271–277.